

## *Retraction*

# **Retracted: Research on Transmission Line Fault Location Based on the Fusion of Machine Learning and Artificial Intelligence**

### **Security and Communication Networks**

Received 26 December 2023; Accepted 26 December 2023; Published 29 December 2023

Copyright © 2023 Security and Communication Networks. This is an open access article distributed under the Creative Commons Attribution License, which permits unrestricted use, distribution, and reproduction in any medium, provided the original work is properly cited.

This article has been retracted by Hindawi, as publisher, following an investigation undertaken by the publisher [1]. This investigation has uncovered evidence of systematic manipulation of the publication and peer-review process. We cannot, therefore, vouch for the reliability or integrity of this article.

Please note that this notice is intended solely to alert readers that the peer-review process of this article has been compromised.

Wiley and Hindawi regret that the usual quality checks did not identify these issues before publication and have since put additional measures in place to safeguard research integrity.

We wish to credit our Research Integrity and Research Publishing teams and anonymous and named external researchers and research integrity experts for contributing to this investigation.

The corresponding author, as the representative of all authors, has been given the opportunity to register their agreement or disagreement to this retraction. We have kept a record of any response received.

### **References**

- [1] X. Liu, "Research on Transmission Line Fault Location Based on the Fusion of Machine Learning and Artificial Intelligence," *Security and Communication Networks*, vol. 2021, Article ID 6648257, 8 pages, 2021.

## Research Article

# Research on Transmission Line Fault Location Based on the Fusion of Machine Learning and Artificial Intelligence

Xiao-Wei Liu 

School of Electrical Engineering and Automation, Wuhan University, Wuhan 430000, China

Correspondence should be addressed to Xiao-Wei Liu; 2014102070013@whu.edu.cn

Received 25 December 2020; Revised 10 January 2021; Accepted 14 February 2021; Published 2 March 2021

Academic Editor: Chi-Hua Chen

Copyright © 2021 Xiao-Wei Liu. This is an open access article distributed under the Creative Commons Attribution License, which permits unrestricted use, distribution, and reproduction in any medium, provided the original work is properly cited.

After a transmission line fails, quickly and accurately find the fault point and deal with it, which is of great significance to maintaining the normal operation of the power system. Aiming at the problems of low accuracy of traditional traveling wave fault location methods and many affected factors, this paper relies on distributed traveling wave monitoring points arranged on transmission lines to study methods to improve the accuracy of traveling wave fault location on transmission lines. First, when a line fails, a traveling wave signal that moves to both ends will be generated and transmitted along the transmission line. We use the Radon transform algorithm to process the traveling wave signal. Then, this paper uses ant colony algorithm to analyze and verify the location and extent of transmission line faults and then optimizes high-precision collection and processing. Finally, the simulation distance measurement is carried out on double-terminal transmission lines and multiterminal transmission lines (T-shaped lines) with branches. The results show that, for double-ended transmission lines, the algorithm increases the speed of matrix calculations and at the same time makes the fault location error of the transmission grid still maintain the improved effect.

## 1. Introduction

Transmission lines bear the heavy responsibility of transmitting electrical energy and are the most extensively distributed component of the power grid [1, 2]. With the gradual construction of the power grid, the total length of long-distance, large-capacity AC and DC transmission lines of various voltage levels are gradually increasing. Most of the overhead transmission lines are erected in the wild, passing through hills, mountains, rivers, and other terrains, and are extremely susceptible to various extreme weather and harsh environments and cause failures [3, 4]. The precise location of the fault point of the transmission line can reduce the manpower and material resources consumed by the line inspection work after the fault and improve the reliability of the power supply [5].

After decades of development and research, the fault barium (distance algorithm) mainly includes the following categories: impedance method, fault analysis method, traveling wave method, frequency-domain method, and artificial intelligence algorithm [6]. Among them,

impedance method and fault analysis method are both short-circuit. After the fault characteristic quantity is analyzed, it is collectively called the fault analysis method [7]. According to different sources of information, the ranging algorithm can be divided into three types: single-ended ranging algorithm, double-ended ranging algorithm, and three-terminal ranging algorithm [8, 9]. According to different models, the ranging algorithm can also be divided into two types: distributed parameter model algorithm and centralized parameter model algorithm. Under the current rapid development trend, the generation and application of the flexible DC transmission technology mentioned above mainly have the following points [10, 11]. The continuous increase of power load makes the existing power transmission system unable to meet the needs of long-distance and large-capacity transmission of electric energy under today's control operation technology [12]. In general, the fault location accuracy of the impedance method and the fault analysis method is lower than that of the line, although the first two methods require low sampling rate and are easy to implement, with the continuous development and

advancement of relay protection technology, the quick-action performance of the protection element is greatly improved, the fault data window is greatly shortened, and the fault location accuracy of the time-domain method based on distributed parameters is not affected by the line and system parameters [13, 14].

After the transmission line fails, quickly and accurately find the fault point and deal with it, which is of great significance for maintaining the normal operation of the power system [15, 16]. Aiming at the problems of low accuracy of traditional traveling wave fault location methods and many affected factors, this paper relies on distributed traveling wave monitoring points arranged on transmission lines to study methods to improve the accuracy of traveling wave fault location on transmission lines and through Radon transform and ant Group algorithms carry out signal processing and data analysis. Damage to power transmission equipment may also cause the overall structure of power transmission and distribution to be paralyzed. Therefore, accurate fault location and troubleshooting has become an important topic for domestic and foreign experts and scholars and has important economic benefits and broad application prospects.

## 2. Overview of Transmission Line Faults

As early as 1969, SANT and Paithankar first proposed a single-ended ranging algorithm, that is, by collecting the voltage and current at one end of the line and calculating the fault distance through a formula [17, 18]. It is feasible to use a single-sided power supply line, but for a double-sided power supply, due to the increase of side auxiliary current and the large transition resistance of the fault point, a large distance deviation will often occur. In the early 1990s, the institute systematically studied current transformers manufactured with traditional technology and conducted many field tests on their transient response characteristics [19, 20].

The test results show that the current transient component can be transmitted through a traditional current transformer. Based on this research, the study of traveling wave faults is mainly aimed at the development of current traveling wave and traveling wave fault location devices, using current traveling wave as a template. In recent years, domestic and foreign experts and scholars have paid more and more attention to the research of fault location. Various ranging methods stand out [21, 22]. Combining physics, advanced mathematics, and other subject knowledge into the research of distance measurement theory promotes the development of distance measurement methods. The schematic diagram of transmission line fault location is shown in Figure 1.

Many researchers introduced related research results, such as statistical probability and statistical decision-making, artificial neural network algorithms, and wavelet transform [23, 24]. In order to achieve economies of scale, reduce network losses, ensure the reliability of the power system, and reduce the impact of transmission lines on power transmission, research on HVDC transmission technology has been carried out one after another at home

and abroad [25]. With the early successful application of HVDC in submarine cable power transmission systems, HVDC power transmission technology has gradually been applied to long-distance, large-scale power transmission systems. The most representative project is the US Pacific Tie Line Project that started operation in 1970. Later, with the invention of the thyristor valve, the HVDC system developed faster [26]. As a carrier of long-distance and large-capacity power transmission, DC transmission lines are as important as the "blood vessels" of the human body but are prone to failures. The control and protection system needs to correctly locate the fault points and take measures after failures. At present, in principle, the fault location methods can be divided into three categories. One is the traveling wave method. The traveling wave method is mainly divided into two different methods. Both can be used to measure the fault distance but have their own advantages and disadvantages [27].

## 3. Transmission Line Fault Handling Based on Ant Colony and Radon Transformation

Radon transformation is a transformation method used to calculate the projection of an image in a specified direction. When the integral path is a straight line, the variable is a linear transformation [28]. The vector always exists because it is obtained through a simple mapping. The simulation model established in this paper is a power system power supply model with a transmission line length of 200 km, a voltage level of 110 kV, and a frequency of 50 Hz. The positive sequence and zero sequence resistance per unit length are  $R1 = 0.027952 \Omega/\text{km}$  and  $R2 = 0.27952 \Omega/\text{km}$ . When  $G$  exists, the above two equations form an inverse transform pair. When the noise is added, the noise is transformed into the Radon domain [29]. Assuming that the data is the result of applying the following algorithm, then the objective function can be minimized, and there are two calculation forms.

When  $|N_x \geq N_p|$ , the least square solution of the problem is

$$\mu = (L^H L)^{-1} L^H d. \quad (1)$$

When  $|N_x < N_p|$ , the minimum norm solution of the problem is

$$\mu = L^H (L^H L)^{-1} d. \quad (2)$$

Generally, the above formulas need to play an anti-overlapping effect and need to provide relatively high resolution in the transform domain. In the process of matrix inversion, singularities often appear, especially for the low-frequency band [30]. For the stability of the forward transformation process, a damping parameter is usually added.

The definition of positive transformation is as follows:

$$\mu(\tau, p) = \int_{-\infty}^{+\infty} d(t = \tau + px, x) dx. \quad (3)$$

The corresponding inverse transformation is defined as

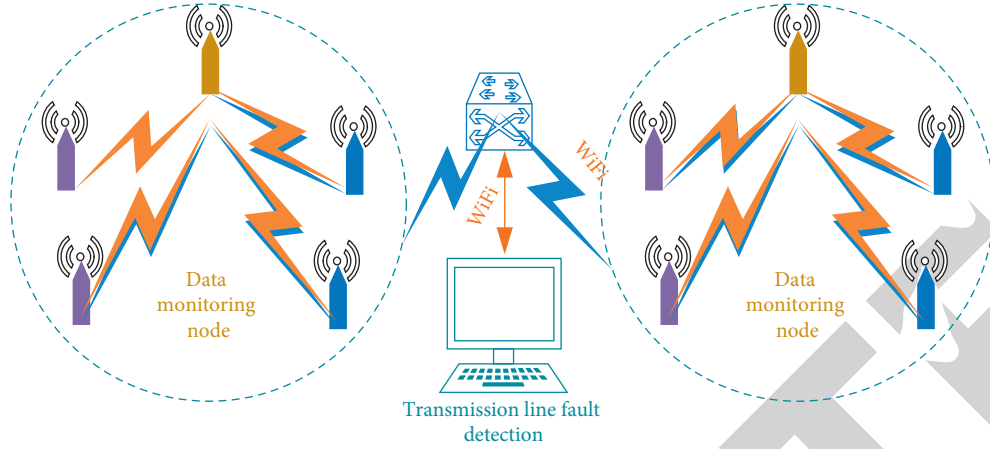


FIGURE 1: Schematic diagram of transmission line fault location.

$$d'(t, x) = \int_{-\infty}^{+\infty} \mu(\tau - px, x) dp. \quad (4)$$

A schematic diagram of the algorithm flow of Radon transform is shown in Figure 2.

The linear discrete form is obtained by adding the integrals in the continuous Radon transform to the finite area. First, suppose that the seismic data have channels, where is the corresponding far offset and near offset, and what is the number of data channels in the radon domain. The discrete form of the positive transformation is

$$\mu(\tau, p) = \sum_i^{N_x} d(t = \tau + px_i, x_i) \Delta x_i. \quad (5)$$

In the formula,  $\Delta x_i = (x_{i+1} - x_i)$ ,  $i \in [0, N_p)$ . The corresponding inverse transformation form is

$$d'(t, x) = \sum_j^{N_p} \mu(\tau = t - p_j x, p_j) \Delta p_j. \quad (6)$$

In the formula,  $\Delta p_j = (p_{j+1} - p_j)$ ,  $j \in [0, N_p)$ . The above two formulas are expressed in matrix form as follows:

$$\mu = L^H d, \quad (7a)$$

$$d' = L\mu. \quad (7b)$$

The above formula represents a pair of conjugate transformation operators. The matrix is a forward transformation operator, which means it is a conjugate operator, that is, an inverse transformation operator.

$$\text{net}_{p_j} = \text{net} = \sum_{i=1}^M \omega_{ij} o_i. \quad (8)$$

The linear superposition operator, as shown in the above formula, maps the data from the spatial domain to the domain

$$o_j = f(\text{net}_j). \quad (9)$$

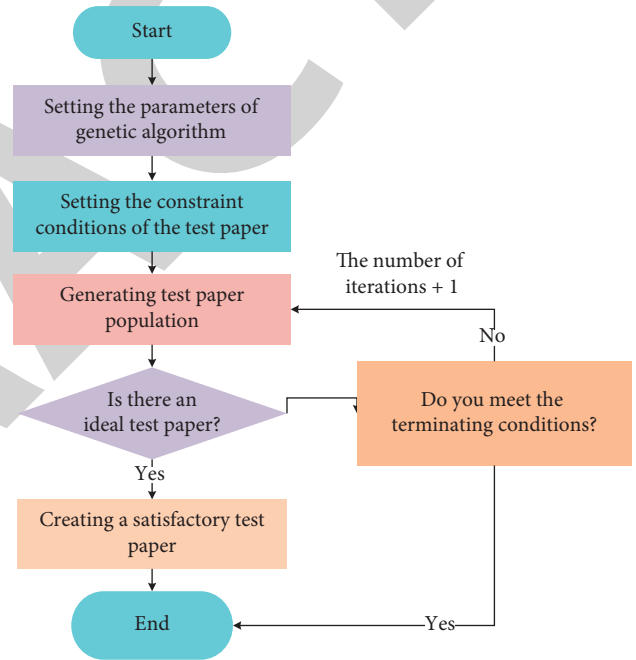


FIGURE 2: Schematic diagram of the algorithm flow of Radon transform.

On the contrary, its conjugate equation (7b) maps the data from the child domain to parent domain. According to different models, the ranging algorithm can also be divided into two types: distributed parameter model algorithm and centralized parameter model algorithm.

$$\text{net}_k = \sum_{j=1}^q \omega_{jk} o_j. \quad (10)$$

Under the current rapid development trend, the generation and application of the flexible DC transmission technology mentioned above mainly have the following points:



$$f(\text{net}_j) = \frac{1}{1 + \exp[-(\text{net}_j - \theta_j)]}. \quad (11)$$

The continuous increase of power load makes the existing power transmission system unable to meet the needs of long-distance and large-capacity transmission of electric energy under today's control operation technology.

$$f'(\text{net}_j) = f(\text{net}_j)[1 - f(\text{net}_j)]. \quad (12)$$

The vector always exists because it is obtained through a simple mapping. The simulation model established in this paper is a power system power supply model with a transmission line length of 200 km, a voltage level of 110 kV, and a frequency of 50 Hz. The control and protection system needs to correctly locate the fault points and take measures after failures. At present, in principle, the fault location methods can be divided into three categories. Some parameters of the task pricing plan in the transmission line signal conversion data are shown in Table 1.

They are nonorthogonal, so they cannot form a reciprocal transform pair. The problem for a given equation is how to recover  $d$ . The relationship between  $d$  and  $t$  can be obtained by substituting formula (7a) into formula (7b).

#### 4. Case Verification of Transmission Line Fault Handling

When adopting the fault location method based on fault type identification, the calculation should be carried out according to the following steps. The first step is to calculate the characteristic quantities of the spatial domain correlation dimension, time-domain difference square root, and multifractal dimension sequence based on the acquired fault voltage signal. The second step is to calculate the weight of the two characteristic quantity indicators of the correlation dimension and the difference square root to obtain the fault signal. The simulation model established in this paper is a power system power supply model with a transmission line length of 200 km, a voltage level of 110 kV, and a frequency of 50 Hz. The positive sequence and zero sequence resistance per unit length are  $R1 = 0.027952 \Omega/\text{km}$  and  $R2 = 0.27952 \Omega/\text{km}$ . The positive sequence and zero sequence conductance per unit length are  $R1 = 0.88 \text{ H}/\text{km}$  and  $R2 = 3.1 \text{ H}/\text{km}$ . The positive sequence and zero sequence capacitance per unit length are  $R1 = 0.0133 \mu\text{F}/\text{km}$  and  $R2 = 0.00875 \mu\text{F}/\text{km}$ .

**4.1. Technical Performance Test.** The traveling wave generated by the fault of the DC transmission line of the MMC-HVDC system is essentially a mixed signal composed of multiple different frequency components. Due to the influence of line parameters, the actual propagation and attenuation speeds of components of different frequencies on the line are different. Therefore, the traveling wave will be distorted in the process of propagation, which greatly increases the difficulty in measuring the time when the faulted traveling wave head reaches the bus bar of the line and determining the polarity of the refracted traveling wave head. Perform fault simulation on the T-type line built by

PSCAD. After the three-terminal fault is measured, obtain the M, N, P three-terminal fault current, as shown in Figure 3. Intercept the fault current of 0.06 s–0.1 s, and carry out Hilbert–Huang transformation according to the fault flow in this paper. The simulation model established in this paper is a power system power supply model with a transmission line length of 200 km, a voltage level of 110 kV, and a frequency of 50 Hz. According to the measured three-terminal traveling wave head, the model data simulated in PSCAD in the previous section is processed, and then, the waveform is imported into MATLAB, and db4 wavelet is used for analysis during simulation. The wavelet transform is performed on the voltage waveforms on both sides of the M and N terminals to obtain the arrival time of the traveling wave head. The measured transformation result is shown in Figure 4.

**4.2. Comparison of Ant Colony Algorithm and Other Algorithms.** Figure 5 shows the wavelet transform result of the voltage traveling wave at the M terminal (the N terminal is similar). As explained in Figure 5, when the intersection method is used to determine whether an insulator has a flashover failure, if the overvoltage curve at both ends of the insulator or the horizontal extension of the curve extreme point intersects its own volt-second characteristic curve, it is judged that the insulator has a flashover failure.

Flashover moment is the abscissa of the intersection of the overvoltage curve or its extreme point horizontal extension line and the volt-second characteristic curve. For overvoltages with similar waveforms, as the amplitude of the overvoltage curve decreases, the flashover time also lags. The application of the modulus maximum has a better removal effect on white noise, especially when there are too many singular points. In addition, it can effectively guarantee the stability of the amount of vibration signal, while saving the effective information in the singularity of the signal. It is a good estimate of the initial signal and has a good picture quality. The effect of double-terminal traveling wave fault location to eliminate wave speed error is shown in Figure 6.

It can be seen from Figure 7 that the fault location error level measured by the fault traveling wave waveform with a sampling frequency of 10 MHz is significantly smaller than the fault location error level measured by the fault traveling wave waveform with a sampling frequency of 1 MHz. In the 12 sets of samples, the maximum error of the fault point position measured by the fault traveling wave waveform with a sampling frequency of 1 MHz is 118 m, and for the fault traveling wave waveform with a sampling frequency of 10 MHz, the measured fault point position is the largest. The error is only 13.2 m. Increasing the sampling frequency by ten times reduces the maximum fault location error by almost an order of magnitude. The original signal and the comparison curve after modulus maximum processing are shown in Figure 8.

This rule is also in line with the theoretical analysis in the previous section. Because the modulus maximum reconstruction is an alternate projection method, the accuracy of the reconstructed signal and the high signal-to-noise ratio

TABLE 1: Some parameters of the task pricing plan in the transmission line signal conversion data.

	$t_1$	$t_2$	$t_3$	$t_4$	...	$t_{831}$	$t_{832}$	$t_{833}$	$t_{834}$	$t_{835}$
$S_{w1}$	0.2250	0.6634	0.3956	0.2366	...	0.1600	0.1890	0.5201	0.4116	0.1623
$S_{w2}$	0.2706	0.6932	0.4210	0.6091	...	0.9176	0.8927	0.6131	1.0080	0.9176
$S_{w3}$	0.6592	0.8512	0.4201	0.6125	...	0.9765	1.0265	0.9763	1.0256	0.9856
$S_{w4}$	0.9437	1.0246	0.4241	0.6393	...	1.0843	1.1076	1.5017	1.0584	1.0843
...	...	...	...	...	...	...	...	...	...	...
$S_{w(n-1)}$	1.5484	1.4033	1.0391	0.8760	...	1.8013	1.8187	1.7916	2.1187	1.8012
$S_{wn}$	1.6566	1.6636	1.6001	1.3904	...	2.2379	2.2105	2.0463	2.2344	2.2379
$S_w$	15.4676	10.2045	3.1821	6.3872	...	1.4607	2.3245	1.0258	0.5027	1.8898
$Q_w$	72.5	69	65.5	80	...	75	71	80	65.5	82

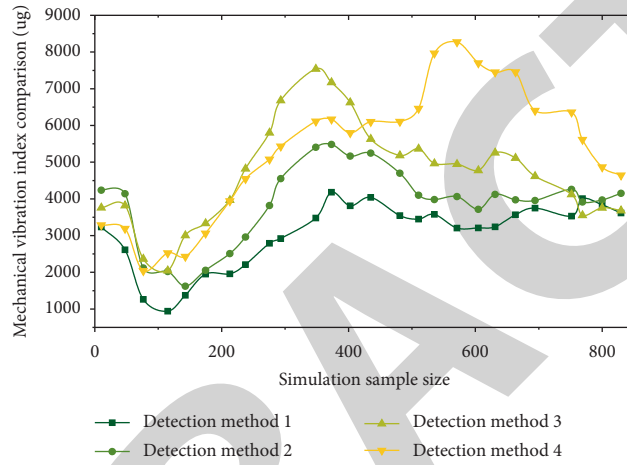


FIGURE 3: M, N, P three-terminal transmission line fault current.

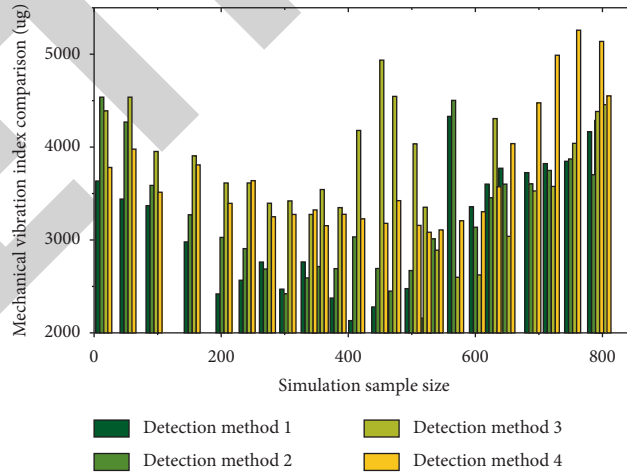


FIGURE 4: Hilbert-Huang transformation results of the fault process.

needs to be guaranteed. Generally, many iterations are required, which makes it more time-consuming than the other two methods. The choice of wavelet decomposition scale is the key point in the process of applying the modulus

maximum method to denoise. Pseudoextreme points will occur when small-scale wavelet coefficients are affected by noise. It is easy to miss important singularity signals at large scales. Therefore, this method is more practical for low

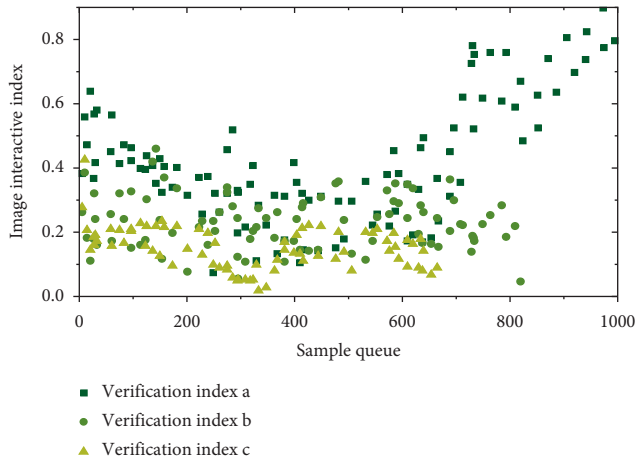


FIGURE 5: Wavelet transform result of voltage traveling wave at M terminal.

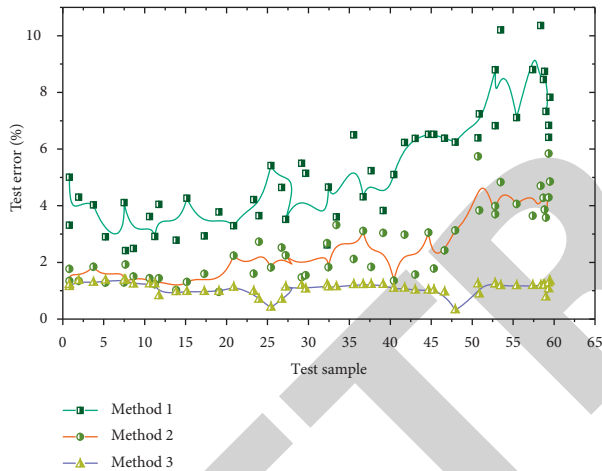


FIGURE 6: The effect of double-terminal traveling wave fault location to eliminate wave speed error.

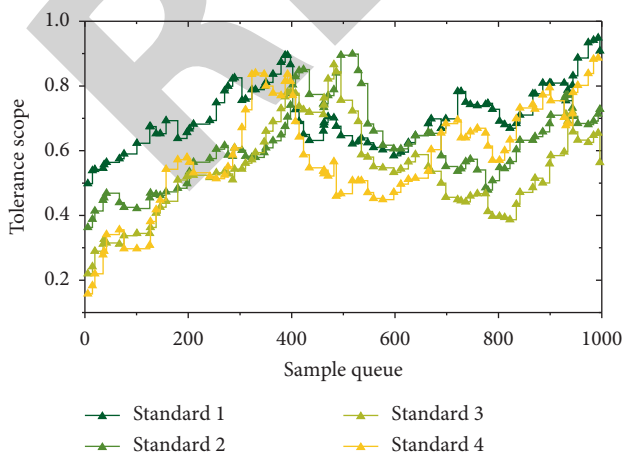


FIGURE 7: The fault traveling wave waveform with a frequency of 10 MHz.

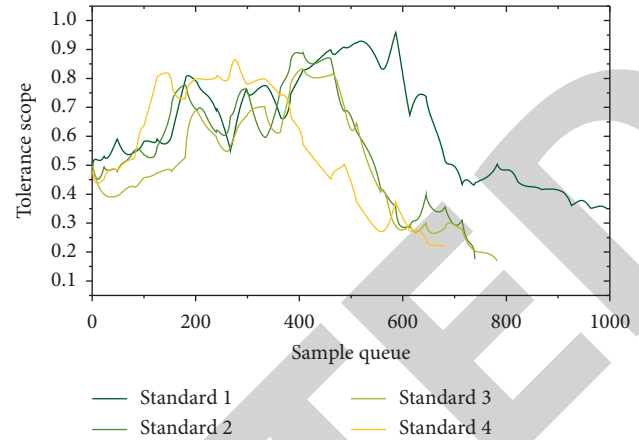


FIGURE 8: The original signal and the comparison curve after modulus maximum processing.

signal-to-noise ratio signals. This shows that when the sampling frequency is low, increasing the sampling frequency of the traveling wave measuring device can significantly improve the accuracy of the traveling wave arrival time detected by the VMD/TEO algorithm, thereby improving the positioning accuracy.

## 5. Conclusion

In this paper, based on the DC transmission system, the ant colony algorithm and Radon transform transmission line fault signal analysis method are proposed, and the method is applied to the fault location of the DC fault and the fault identification of the commutation failure. After the transmission line fails, quickly and accurately find the fault point and deal with it, which is of great significance for maintaining the normal operation of the power system.

Aiming at the problems of low accuracy of traditional traveling wave fault location methods and many affected factors, this paper relies on distributed traveling wave monitoring points arranged on transmission lines to study methods to improve the accuracy of traveling wave fault location on transmission lines. First, when a line fails, a traveling wave signal that moves to both ends will be generated and transmitted along the transmission line. We use the Radon transform algorithm to process the traveling wave signal. Then, this paper uses ant colony algorithm to analyze and verify the location and extent of transmission line faults and then optimizes high-precision collection and processing. Finally, the simulation distance measurement is carried out on double-terminal transmission lines and multiterminal transmission lines (T-shaped lines) with branches. The results show that, for double-ended transmission lines, the algorithm increases the speed of matrix calculations and at the same time makes the fault location error of the transmission grid still maintain the improved effect. The combination of ant colony algorithm and Radon transform can realize line fault location and commutation failure fault identification. However, this method uses the energy of different nodes as fault characteristics for different faults, and the output of the network is different. In the

follow-up, the feature vector extraction of the two faults needs to be further integrated and unified to simplify the control and protection system.

## Data Availability

The data used to support the finding of this study are included in the article.

## Conflicts of Interest

The author declares no conflicts of interest or personal relationships that could have appeared to influence the work reported in this paper.

## References

- [1] X. Zheng, S. Zhou, and H. Chen, "Ant colony optimisation algorithms for two-stage permutation flow shop with batch processing machines and nonidentical job sizes," *International Journal of Production Research*, vol. 57, no. 9-10, pp. 3060–3079, 2019.
- [2] Z. Zhang, F. Hu, and N. Zhang, "Ant colony algorithm for satellite control resource scheduling problem," *Applied Artificial Intelligence*, vol. 48, no. 10, pp. 3295–3305, 2018.
- [3] K. Yaghoobirafi and E. Nazemi, "An approach to XBRL interoperability based on Ant Colony Optimization algorithm," *Knowledge-Based Systems*, vol. 163, no. 1, pp. 342–357, 2019.
- [4] M. Stumpe, P. Ruffing, P. Wagner, and A. Schnettler, "Adaptive single-Pole autoreclosing concept with advanced DC fault current control for full-bridge MMC VSC systems," *Institute of Electrical and Electronics Engineers Transactions on Power Delivery*, vol. 33, no. 1, pp. 321–329, 2018.
- [5] N. Shweta, N. Kishor, K. Uhlen, and S. R. Mohanty, "Detecting instant of multiple faults on transmission line and its types using time-frequency analysis," *IET Generation Transmission & Distribution*, vol. 13, no. 22, pp. 5248–5256, 2019.
- [6] P. R. Shrestha, N. Abhyankar, M. A. Anders et al., "Non-resonant transmission line probe for sensitive interferometric electron spin resonance detection," *Analytical Chemistry*, 2019.
- [7] X. Shi, F. Xie, and B. Zhang, "S. O. Automation, H. D. university, a global approach to manned submersibles based on improved ant colony optimization algorithm," *Ocean Engineering*, 2019.
- [8] B. Patel and P. Bera, "Fast fault detection during power swing on a hybrid transmission line using wavelet packet transform," *IET Generation Transmission & Distribution*, vol. 13, no. 10, 2019.
- [9] J. Ning, Q. Zhang, C. Zhang, and B. Zhang, "A best-path-updating information-guided ant colony optimization algorithm," *Information Sciences*, vol. 433-434, pp. 142–162, 2018.
- [10] S. Moon, "Orthogonal function series formulas for inversion of the spherical Radon transform," *Inverse Problems*, vol. 36, no. 3, p. 17, Article ID 035007, 2020.
- [11] S. Moon, "Orthogonal function series formulae for inversion of the conical Radon transform with a fixed central axis," *Inverse Problems*, vol. 35, no. 12, Article ID 125007, 2019.
- [12] L. M. N. D. Mattos, M. C. Tavares, and A. M. P. Mendes, "A new fault detection method for single-phase Auto-reclosing," *Institute of Electrical and Electronics Engineers Transactions on Power Delivery*, vol. 33, no. 6, pp. 2874–2883, 2018.
- [13] Y. Luo, Y. Yang, K. Zhao, Y. Xu, and J. Xia, "Unraveling overtone interferences in Love-wave phase velocity measurements by radon transform," *Geophysical Journal International*, vol. 203, pp. 327–333, 2018.
- [14] S. Lu, "Multi-objective workshop scheduling of marine production based on improved ant colony algorithm," *Journal of Coastal Research*, vol. 107, no. 1, p. 222, 2020.
- [15] Q. Liao, Y. Guo, Y. Tu, and H. Zhang, "Fidelity-based ant colony algorithm with Q-learning of quantum system," *International Journal of Theoretical Physics*, vol. 57, no. 3, pp. 862–876, 2018.
- [16] Q. Liang, W. Ouyang, W. Mao, and S. Cheng, "Scattering pattern analysis and true amplitude generalized Radon transform migration for acoustic transversely isotropic media with a vertical axis of symmetry," *Geophysical Prospecting*, vol. 68, no. 4, pp. 1211–1227, 2020.
- [17] Z. Li, N. Tong, X. Lin et al., "Enhanced summation impedance relay for EHV transmission lines," *Institute of Electrical and Electronics Engineers Transactions on Power Delivery*, vol. 34, no. 3, pp. 807–818, 2019.
- [18] Y. Li, L. Wu, J. Li et al., "DC fault detection in MTDC systems based on transient high frequency of current," *Institute of Electrical and Electronics Engineers Transactions on Power Delivery*, vol. 34, no. 3, pp. 950–962, 2019.
- [19] J. Li, Q. Yang, H. Mu, S. Le Blond, and H. He, "A new fault detection and fault location method for multi-terminal high voltage direct current of offshore wind farm," *Applied Energy*, vol. 220, no. 15, pp. 13–20, 2018.
- [20] B. Khorram and M. Yazdi, "A new optimized thresholding method using ant colony algorithm for MR brain image segmentation," *Journal of Digital Imaging*, vol. 32, no. 1, pp. 162–174, 2019.
- [21] A. Katsevich, "Resolution analysis of inverting the generalized radon transform from discrete data in  $\mathbb{R}^3$ ," *Siam Journal on Mathematical Analysis*, vol. 52, no. 4, pp. 3990–4021, 2020.
- [22] M. Greenblatt, "Smooth and singular maximal averages over 2D hypersurfaces and associated Radon transforms," *Advances in Mathematics*, vol. 377, Article ID 107465, 2020.
- [23] S. Gangolu, P. Raja, M. P. Selvan, and V. K. Murali, "Effective algorithm for fault discrimination and estimation of fault location in transmission lines," *IET Generation, Transmission & Distribution*, vol. 13, no. 13, pp. 2789–2798, 2019.
- [24] X. Ding, S. Zhang, H. Li, P. Wu, and S. Cheng, "A restrictive polymorphic ant colony algorithm for the optimal band selection of hyperspectral remote sensing images," *International Journal of Remote Sensing*, vol. 2, pp. 1–25, 2019.
- [25] A. Cozza, "Never trust a cable bearing echoes: understanding ambiguities in time-domain reflectometry applied to soft faults in cables," *Institute of Electrical and Electronics Engineers Transactions on Electromagnetic Compatibility*, vol. 61, no. 2, pp. 586–589, 2019.
- [26] J. Chia-Feng, C.-H. Lin, and T. B. Bui, "Multiobjective rule-based cooperative continuous ant colony optimized fuzzy systems with a robot control application," *Institute of Electrical and Electronics Engineers Transactions on Cybernetics*, vol. 50, no. 2, pp. 650–663, 2018.
- [27] Y. Q. Chen, J. L. Guo, H. Yang, Z. Q. Wang, and H. L. Liu, "Research on navigation of bidirectional A\* algorithm based on ant colony algorithm," *Journal of Supercomputing*, vol. 1, 2020.
- [28] S. Chaouch, A. Moussa, I. B. Marzoug, and N. Ladhari, "Colour recipe prediction using ant colony algorithm:



- principle of resolution and analysis of performances,” *Collaboration Technology*, vol. 135, no. 5, 2019.
- [29] G. Ambartsoumian and E. T. Quinto, “Generalized Radon transforms and applications in tomography,” *Inverse Problems*, vol. 36, no. 2, Article ID 020301, 2020.
- [30] M. Aharchaou and A. Levander, “A compressive sensing approach to the high-resolution linear Radon transform: application on teleseismic wavefields,” *Geophysical Journal International*, vol. 207, no. 2, pp. 811–822, 2018.

RETRACTED